Continuum Mech. Thermodyn.
https://doi.org/10.1007/s00161-021-01034-y

ORIGINAL ARTICLE

Mohammad Malikan · **Victor A. Eremeyev**

Flexomagneticity in buckled shear deformable hard-magnetic soft structures

Received: 4 March 2021 / Accepted: 8 June 2021

Abstract This research work performs the first time exploring and addressing the flexomagnetic property in a shear deformable piezomagnetic structure. The strain gradient reveals flexomagneticity in a magnetization phenomenon of structures regardless of their atomic lattice is symmetrical or asymmetrical. It is assumed that a synchronous converse magnetization couples both piezomagnetic and flexomagnetic features into the material structure. The mathematical modeling begins with the Timoshenko beam model to find the governing equations and non-classical boundary conditions based on shear deformations. Flexomagneticity evolves at a small scale and dominant at micro/nanosize structures. Meanwhile, the well-known Eringen's-type model of nonlocal strain gradient elasticity is integrated with the mathematical process to fulfill the scaling behavior. From the viewpoint of the solution, the displacement of the physical model after deformation is carried out as the analytical solution of the Galerkin weighted residual method (GWRM), helping us obtain the numerical outcomes on the basis of the simple end conditions. The best of our achievements display that considering shear deformation is essential for nanobeams with larger values of strain gradient parameter and small amounts of the nonlocal coefficient. Furthermore, we showed that the flexomagnetic (FM) effect brings about more noticeable shear deformations' influence.

Keywords Flexomagneticity · Buckling analysis · Timoshenko nanobeam · NSGT · GWRM

List of symbols

ε_{xx}	Axial strain
γ_{xz}	Shear strain
η_{xxz}	Gradient of the axial elastic strain
C_{11}	Elastic modulus
σ_{xx}	Axial stress
τ_{xz}	Shear stress

Communicated by Andreas Öchsner.

M. Malikan (✉) · V. A. Eremeyev
Department of Mechanics of Materials and Structures, Faculty of Civil and Environmental Engineering, Gdansk University of Technology, 80-233 Gdansk Gdansk, Poland
E-mail: mohammad.malikan@pg.edu.pl; mohammad.malikan@yahoo.com

V. A. Eremeyev
Don State Technical University, Gagarina sq., 1, Rostov on Don, Russia 344000

V. A. Eremeyev
DICAAR, Università degli Studi di Cagliari, Via Marengo, 2, 09123 Cagliari, Italy

Published online: 25 June 2021

f_{31}	Component of the fourth-order flexomagnetic coefficients tensor
a_{33}	Component of the second-order magnetic permeability tensor
q_{31}	Component of the third-order piezomagnetic tensor
ξ_{xxz}	Component of the higher-order hyper-stress tensor
B_z	Magnetic flux
H_z	Component of magnetic field
g_{31}	Influence of the sixth-order gradient elasticity tensor
q	Third-order piezomagnetic tensor
a	Second-order magnetic permeability tensor
g	sixth-order gradient elasticity tensor
C	Fourth-order elasticity coefficient tensor
f	Fourth-order flexomagnetic tensor
r	Fifth-order tensor
$u_i (i = 1, 3)$	Displacement in the x and z directions
u and w	Axial and transverse displacements of the mid-plan
ϕ	Rotation of beam elements around the y axis
z	Thickness coordinate
ψ	External magnetic potential
Ψ	Magnetic potential function
l (nm)	Strain gradient length scale parameter
μ (nm)$^2 = (e_0 a)^2$	Nonlocal parameter
X_m	Residue of the equations
k_s	Shear correction factor
N_x	Axial stress resultant
Q_x	Shear stress resultant
M_x	Moment stress resultant
T_{xxz}	Hyper stress resultant

1 Introduction

Magnetic properties are divided into different categories: diamagnetic, paramagnetic, ferrimagnetic ferromagnetic materials, etc. Ferromagnetic materials are magnetic structures with high permeability such as cobalt and iron Ferromagnetic materials are divided into hard (e.g., $CoFe_2O_4$) and soft groups (e.g. Fe_3O_4). Hard magnetic materials are materials that become magnetized hardly ever; that is, a strong magnetic field is required to create magnetism in them. As these materials become magnetized hardly, they also lose scarcely ever their magnetic properties. These structures are suited to be used as a steady magnetic state such as sensors and measuring instruments. Conversely, soft magnetic structures are easily magnetized and just as easily lose their magnetic properties [1–5]

$CoFe_2O_4$ magnetic nanostructures have received particular attention among different spinel ferrites, such as exclusive physical features excellent mechanical hardness, significant magnetostrictive coefficient, high coercivity, moderate saturation magnetization, etc. [6,7] From a technological perspective, these characteristic properties cause the structure described above entirely significant, leading to its application in gas sensors, magnetic hyperthermia, biosensors, ferrofluid technology, and high-density magnetic media [8–11].

A lot of practical applications can be observed from the phenomenological magneto-mechanical coupling of crystals. Structures with reduced dimensions functioning as nano configurations are affected principally and importantly from this type of coupling. It is already known that the connection between induced magnetization and strain gradient is mainly significant among smallsize structures Flexomagneticity (FM) is a phenomenon that exists during the magneto-mechanical coupling regarding the magnetic field and strain gradient [12–14]. Compared to the flexomagneticity, flexoelectricity influence appears in crystalline structures between the electric field and strain gradient (converse effect) [15–33]. The physical action of FM makes it competent to the economic outlook The advantage of FM property gives a possible way of improving biosensor efficiency

The contemporary decade has been witnessed plenty of research work performed on the mechanics of piezomagnetic (PM) nano configurations [34–42]. However, the availability of FM in scientific papers is seen hardly and scarcely [43–52]. In the aforementioned reports presented on FM for PM structures, in order to model the domain displacement field, all available references employed the concept of the Euler–Bernoulli

(EB) approach regardless of shear deformation. By contrast, in the present research work, we analyze the transverse shear deformation on the basis of utilizing the Timoshenko beam approach. As long as the domain is a nanoscale volume, the size-dependent mechanical response should be considered. The literature in [43,44] used the surface elasticity hypothesis to address this scale-dependent reaction. Oppositely, in the current paper and similar to [45–52], we handle stress/straindriven non-classical elasticity models conforming to the nonlocal strain gradient size-dependent approach. Using this approach leads to investigating two concurrent size-dependent nanomaterials' behaviors: inhomogeneity distribution of atoms (material particles) and long-range lattice interactions The first one occurs due to a large surface to the volume of atoms and the second one arises concerning the long-range interatomic interaction among the whole atoms of the domain. It is germane to note that the [43,44] applied both direct and converse magnetic fields; however, [45–52] and the present article have taken the converse effect only. We keep the ends of the magnetic nanobeam mathematically in simply-supported boundary conditions through a numerical solving procedure. Up to our knowledge, the literature has confirmed that FM behavior is completely size-dependent.

Moreover, the crucial achievements of [45–52] approved that the FM can cause more material stiffness. Therefore, we aim to investigate the relevance between transverse shear deformation and the FM, which is a novel study in the present scientific work and what follows In a point of fact, until now the FM has been investigated on thin beam models only regardless of shear deformation [43–52]. Furthermore, the linear mathematical model which is obtained by this study is solved through the medium of the Galerkin weighted residual method The numerical results have appeared in line with the graphical figures and detailed parametric diagrams.

2 Mathematical modeling

2.1 Fundamental calculations of the piezomagneticflexomagnetic (PFM) media

We begin the fundamental formulation of a PFM solid by assuming some restrictions acting as minute deformations in an isothermal environment, referencing [12–14]. Thus, the magnetic field H and displacement u are variables in the vector framework

$$u = u\,(x)\,, \quad H = H\,(x) \tag{1}$$

in which x defines a position vector.

We introduce the free energy density U defined within the flexomagneticity as follows

$$\begin{aligned} U = U\,(\varepsilon, \eta, H) = &-\frac{1}{2} H \cdot a \cdot H + \frac{1}{2}\varepsilon : C : \varepsilon + \frac{1}{2}\eta \dot{:} g \dot{:} \eta + \varepsilon : r \dot{:} \eta \\ &- H \cdot q : \varepsilon - H \cdot f \dot{:} \eta \end{aligned} \tag{2}$$

in which "$\dot{:}$", ":", and "$\cdot$" depict the inner (scalar) products in the spaces of third-order tensor, second-order tensor and vectors, respectively.

The elastic strain and its gradient are expressed as

$$\varepsilon = \frac{1}{2}\left(\nabla u + \nabla u^T\right), \quad \eta = \nabla \varepsilon \tag{3}$$

where ∇ is the 3D nabla operator

In what follows, we use the magnetic potential ψ related with H as

$$H = -\nabla \psi \tag{4}$$

To study the FM on a static PM model, based on the virtual work principle, one can use the variational approach

$$\int_V \delta U \mathrm{d}V = \delta A \tag{5}$$

where δA is dedicated for performing the work of outer loads, Vexhibits the domain volume occupied by FM solid.

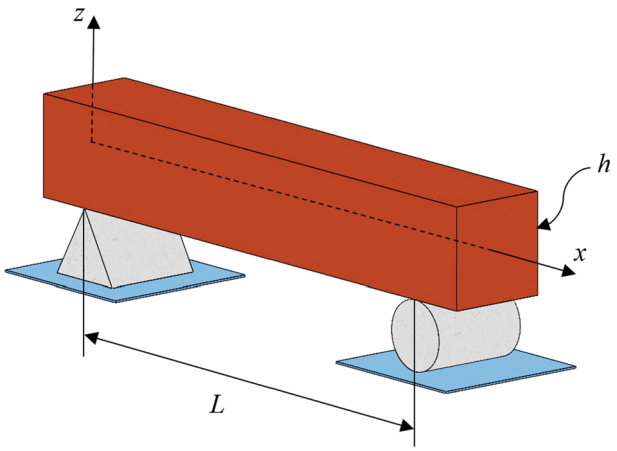

Fig. 1 Geometrical details of a simply supported square figured beam

For simplicity, a standard relation for δA is introduced as

$$\delta A = \int_V F \cdot \delta u + \int_{\partial V} t \cdot \delta u \mathrm{d}s \tag{6}$$

in which t and F display the surface traction and external mass forces, respectively.

We illustrate the following equations based on Eq. (5) and calculus of variations

$$\nabla \cdot (\sigma - \nabla \cdot \xi) + F = 0 \tag{7a}$$
$$\nabla \cdot B = 0 \tag{7b}$$

where B is a magnetic induction vector, and the constitutive relations of a PFM media can be established as

$$\sigma = \frac{\partial U}{\partial \varepsilon} \equiv C : \varepsilon + r \dot{:} \eta - H \cdot q \tag{8a}$$
$$\xi = \frac{\partial U}{\partial \eta} \equiv g : \eta + \varepsilon : r - H \cdot f \tag{8b}$$
$$B = -\frac{\partial U}{\partial H} = a \cdot H + q : \varepsilon + f \dot{:} \eta \tag{8c}$$

2.2 The PFM hard magnetic soft one-dimensional structure

This research tries to develop the FM studies on PM solids by accounting for the shear deformation of the structure while both ends of the one-dimensional beam-shaped configuration are held in simple supports. Regarding Fig. 1, a one-dimensional figured beam bridged by simple ends can be detected. Dimensions of the beam are respectively assigned in the parametric framework by h and L for its thickness and effective length.

While a beam incorporates FM properties, the constitutive relations (Eq. 8) are re-defined as follows [43,44]

$$\sigma_{xx} = C_{11}\varepsilon_{xx} - q_{31}H_z \tag{9}$$
$$\xi_{xxz} = g_{31}\eta_{xxz} - f_{31}H_z \tag{10}$$
$$B_z = a_{33}H_z + q_{31}\varepsilon_{xx} + f_{31}\eta_{xxz} \tag{11}$$

As the main scope of this paper is exerting transverse shear deformation in the PFM solid, we use the Timoshenko model as follows [53,54]

$$u_1(x,z) = u(x) + z\phi(x) \tag{12a}$$
$$u_3(x,z) = w(x) \tag{12b}$$

In view of Lagrangian strain and as the present study addresses the linear stability of PFM nanoscale beams thus

$$\varepsilon_{ij} = \frac{1}{2}\left(\frac{\partial u_i}{\partial x_j} + \frac{\partial u_j}{\partial x_i}\right) \tag{13}$$

On developing Eq. (13) based on Eq. (12), one obtains

$$\varepsilon_{xx} = \frac{\mathrm{d}u}{\mathrm{d}x} + z\frac{\mathrm{d}\phi}{\mathrm{d}x} \tag{14a}$$

$$\gamma_{xz} = \phi + \frac{\mathrm{d}w}{\mathrm{d}x} \tag{14b}$$

$$\eta_{xxz} = \frac{\mathrm{d}\varepsilon_{xx}}{\mathrm{d}z} = \frac{\mathrm{d}\phi}{\mathrm{d}x} \tag{14c}$$

Modifying the Lagrange principle (5) we came to

$$\delta \int (\Pi_W + \Pi_U) = 0 \tag{15}$$

where the given letters Π_U and Π_W state respectively the internal strain energy originated from mechanical and magnetic sections, and mechanical work of external elements accomplished on the system.

The following relation can depict the whole strain energy of the beam

$$\delta\Pi_U = \int_V (\sigma_{xx}\delta\varepsilon_{xx} + \tau_{xz}\delta\gamma_{xz} + \xi_{xxz}\delta\eta_{xxz} - B_z\delta H_z)\,\mathrm{d}V \tag{16}$$

Equilibrium equations and non-classical end supports conditions can be obtained after imposing the variational method on Eq. (16) as follows

$$\delta\Pi_{U_1}^{\mathrm{Mech}} = -\int_0^L \left(\frac{\mathrm{d}N_x}{\mathrm{d}x}\delta u + \frac{\mathrm{d}Q_x}{\mathrm{d}x}\delta w - Q_x\delta\varphi + \frac{\mathrm{d}M_x}{\mathrm{d}x}\delta\varphi + \frac{\mathrm{d}T_{xxz}}{\mathrm{d}x}\delta\varphi\right)\mathrm{d}x \tag{17a}$$

$$\delta\Pi_{U_2}^{\mathrm{Mag}} = -\int_0^L \int_{-h/2}^{h/2} \frac{\mathrm{d}B_z}{\mathrm{d}z}\delta\Psi\,\mathrm{d}z\mathrm{d}x \tag{17b}$$

$$\delta\Pi_{U_1}^{\mathrm{Mech}} = (N_x\delta u + Q_x\delta w + M_x\delta\varphi + T_{xxz}\delta\varphi)|_0^L \tag{18a}$$

$$\delta\Pi_{U_2}^{\mathrm{Mag}} = \int_0^L (B_z\delta\Psi)|_{-h/2}^{h/2}\,\mathrm{d}x \tag{18b}$$

where indices 1 and 2, respectively associated with the mechanical and magnetic parts, furthermore

$$N_x = \int_{-h/2}^{h/2} \sigma_{xx}\mathrm{d}z \tag{19}$$

$$M_x = \int_{-h/2}^{h/2} \sigma_{xx}z\mathrm{d}z \tag{20}$$

$$Q_x = k_s\int_{-h/2}^{h/2} \tau_{xz}\mathrm{d}z \tag{21}$$

$$T_{xxz} = \int_{-h/2}^{h/2} \xi_{xxz} \mathrm{d}z \tag{22}$$

Taking external items such as loads and environmental effects results in mechanical work in the solid, hence [55–58]

$$\Pi_W = \frac{1}{2} \int_0^L N_x^0 \left(\frac{\mathrm{d}w}{\mathrm{d}x} \right)^2 \mathrm{d}x \tag{23}$$

Then, the first variation of Eq. (23) can be produced as

$$\delta \Pi_W = \int_0^L \left(N_x^0 \frac{\mathrm{d}\delta w}{\mathrm{d}x} \frac{\mathrm{d}w}{\mathrm{d}x} \right) \mathrm{d}x \tag{24}$$

where N_x^0 reveals in-plane pre-buckling force.

There is only a transverse component for the present media for the magnetic field determined as [59,60]

$$H_z + \frac{\mathrm{d}\Psi}{\mathrm{d}z} = 0 \tag{25}$$

Let us match the literature and embed the beam in a magnetic potential difference circuit so that the maximum and minimum magnetic potentials are at the uppermost and lowest surfaces, respectively. Therefore, the magnetic boundary conditions for a reverse PM impact besides closedcircuit yields [43,44]

$$\Psi \left(+\frac{h}{2} \right) = \psi, \quad \Psi \left(-\frac{h}{2} \right) = 0 \tag{26a-b}$$

By combining Eqs. (11), (17b), (18b), (25) and (26) together and making some mathematical processes give the magnetic potential distribution in line with the thickness and component of the magnetic field as

$$\Psi = \frac{q_{31}}{2a_{33}} \left(z^2 - \frac{h^2}{4} \right) \frac{\mathrm{d}\phi}{\mathrm{d}x} + \frac{\psi}{h} \left(z + \frac{h}{2} \right) \tag{27}$$

$$H_z = -z \frac{q_{31}}{a_{33}} \frac{\mathrm{d}\phi}{\mathrm{d}x} - \frac{\psi}{h} \tag{28}$$

The study of the structural properties of nanodomains, especially the accurate measurement of their mechanical response, has required complex tools. The ultrasmall size space is transferred into a continuum solid media through some mathematical theorems to avoid using complicated equipment. These theoretical models can act in two forms, integral or differential operators. However, we here employ a differential framework of one of these models, which is famed as nonlocal strain gradient elasticity theory (NSGT) [61]

$$\left(1 - \mu \frac{\mathrm{d}^2}{\mathrm{d}x^2} \right) \sigma_{ij} = C_{ijkl} \left(1 - l^2 \frac{\mathrm{d}^2}{\mathrm{d}x^2} \right) \varepsilon_{ij} \tag{29}$$

In other words, in constitutive relations for stress tensor (8a) we consider C as an integro-differential operator related to Eq. (29).

The right side of the NSGT relation is assumed to project the strain gradient role. This part is significant in the mechanics of micro/nanoscale deformable materials [62]. Further, the left side is considered to render the nonlocality of atoms. Both parts involve extra parameters respectively μ as a nonlocal parameter and l as a strain gradient parameter. It should be reminded that $\mu\,(nm)^2 = (e_0 a)^2$ where e denotes a nonlocal quantity and a indicates a characteristic internal length which can be the distance between the center of two neighbor atoms. It should be remembered that the values of smallscale parameters that existed in NSGT vary in light of several cases, such as the type of end supports In general, the values of these factors are not constant or an associated value for each material [63–66].

Putting Eqs. (14) and (27, 28) into Eqs. (9–11), and combining the obtained relations with Eq. (29), then, respectively, the components of magnetic induction, axial stress, and shear stress can be obtained as

$$\left(1-\mu\frac{\mathrm{d}^2}{\mathrm{d}x^2}\right)\xi_{xxz}=\left(1-l^2\frac{\mathrm{d}^2}{\mathrm{d}x^2}\right)\left[\left(g_{31}+\frac{q_{31}f_{31}z}{a_{33}}\right)\frac{\mathrm{d}\phi}{\mathrm{d}x}+\frac{f_{31}\psi}{h}\right] \tag{30}$$

$$\left(1-\mu\frac{\mathrm{d}^2}{\mathrm{d}x^2}\right)\sigma_{xx}=\left(1-l^2\frac{\mathrm{d}^2}{\mathrm{d}x^2}\right)\left[C_{11}\frac{\mathrm{d}u}{dx}+z\left(C_{11}+\frac{q_{31}^2}{a_{33}}\right)\frac{\mathrm{d}\phi}{\mathrm{d}x}+\frac{q_{31}\psi}{h}\right] \tag{31}$$

$$\left(1-\mu\frac{\mathrm{d}^2}{\mathrm{d}x^2}\right)\tau_{xz}=\left(1-l^2\frac{\mathrm{d}^2}{\mathrm{d}x^2}\right)\left[GA\left(\phi+\frac{\mathrm{d}w}{\mathrm{d}x}\right)\right] \tag{32}$$

Nonlocal stress resultants can be obtained by substituting Eqs. (30–32) into Eqs. (19–22) [67–75]

$$\left(1-\mu\frac{\mathrm{d}^2}{\mathrm{d}x^2}\right)N_x=\left(1-l^2\frac{\mathrm{d}^2}{\mathrm{d}x^2}\right)\left\{I_1\frac{\mathrm{d}u}{\mathrm{d}x}+I_4\right\} \tag{33}$$

$$\left(1-\mu\frac{\mathrm{d}^2}{\mathrm{d}x^2}\right)M_x=\left(1-l^2\frac{\mathrm{d}^2}{\mathrm{d}x^2}\right)\left\{(I_2+I_3)\frac{\mathrm{d}\phi}{\mathrm{d}x}\right\} \tag{34}$$

$$\left(1-\mu\frac{\mathrm{d}^2}{\mathrm{d}x^2}\right)Q_x=\left(1-l^2\frac{\mathrm{d}^2}{\mathrm{d}x^2}\right)\left\{H_{44}\left(\phi+\frac{\mathrm{d}w}{\mathrm{d}x}\right)\right\} \tag{35}$$

$$\left(1-\mu\frac{\mathrm{d}^2}{\mathrm{d}x^2}\right)T_{xxz}=\left(1-l^2\frac{\mathrm{d}^2}{\mathrm{d}x^2}\right)\left\{I_5\frac{\mathrm{d}\phi}{\mathrm{d}x}+I_6\right\} \tag{36}$$

in which the numerical expressions bring about

$$\{I_1,I_2\}=\int_{-h/2}^{h/2}C_{11}\left\{1,z^2\right\}\mathrm{d}z,\quad I_3=\int_{-h/2}^{h/2}\frac{q_{31}^2z^2}{a_{33}}\mathrm{d}z,\quad I_4=\int_{-h/2}^{h/2}\frac{\psi q_{31}}{h}\mathrm{d}z,$$
$$I_5=\int_{-h/2}^{h/2}g_{31}\mathrm{d}z,\quad I_6=\int_{-h/2}^{h/2}\frac{\psi f_{31}}{h}\mathrm{d}z,\quad H_{44}=k_s\int_{-h/2}^{h/2}GA\mathrm{d}z$$

After implementing Eqs. (17a) and (24) in Eq. (15), the equations which govern the PFM beam-shaped solid can be developed by which the beam behaves statically in a local domain

$$\frac{\mathrm{d}N_x}{\mathrm{d}x}=0 \tag{37}$$

$$\frac{\mathrm{d}Q_x}{\mathrm{d}x}+N_x^0\frac{\mathrm{d}^2w}{\mathrm{d}x^2}=0 \tag{38}$$

$$\frac{\mathrm{d}M_x}{\mathrm{d}x}+\frac{\mathrm{d}T_{xxz}}{\mathrm{d}x}-Q_x=0 \tag{39}$$

This is the time to simplify Eqs. (33–36) in the nonlocal domain. To do this, by way of Eqs. (37–39), one can derive

$$N_x=\left(1-l^2\frac{\mathrm{d}^2}{\mathrm{d}x^2}\right)\left\{I_1\frac{\mathrm{d}u}{\mathrm{d}x}+I_4\right\} \tag{40}$$

$$M_x=-\mu\left(I_5\frac{\mathrm{d}^3\phi}{\mathrm{d}x^3}+N_x^0\frac{\mathrm{d}^2w}{\mathrm{d}x^2}\right)+\left(1-l^2\frac{\mathrm{d}^2}{\mathrm{d}x^2}\right)\left\{(I_2+I_3)\frac{\mathrm{d}\phi}{\mathrm{d}x}\right\} \tag{41}$$

$$Q_x=-\mu\left(N_x^0\frac{\mathrm{d}^3w}{\mathrm{d}x^3}\right)+\left(1-l^2\frac{\mathrm{d}^2}{\mathrm{d}x^2}\right)\left\{H_{44}\left(\phi+\frac{\mathrm{d}w}{\mathrm{d}x}\right)\right\} \tag{42}$$

$$T_{xxz}=\left(1-\mu\frac{\mathrm{d}^2}{\mathrm{d}x^2}\right)\left(I_5\frac{\mathrm{d}\phi}{\mathrm{d}x}+I_6\right) \tag{43}$$

Let us re-write Eqs. (37–39) based on Eqs. (40–42) as

$$\left(1-l^2\frac{\mathrm{d}^2}{\mathrm{d}x^2}\right)\left\{I_1\frac{\mathrm{d}^2u}{\mathrm{d}x^2}\right\}=0 \tag{44}$$

$$\left(1-\mu\frac{\mathrm{d}^2}{\mathrm{d}x^2}\right)\left\{N_x^0\frac{\mathrm{d}^2w}{\mathrm{d}x^2}\right\}+\left(1-l^2\frac{\mathrm{d}^2}{\mathrm{d}x^2}\right)\left\{H_{44}\left(\frac{\mathrm{d}\phi}{\mathrm{d}x}+\frac{\mathrm{d}^2w}{\mathrm{d}x^2}\right)\right\}=0 \tag{45}$$

$$\left(1-\mu\frac{\mathrm{d}^2}{\mathrm{d}x^2}\right)\left\{I_5\frac{\mathrm{d}^2\phi}{\mathrm{d}x^2}\right\}-\left(1-l^2\frac{\mathrm{d}^2}{\mathrm{d}x^2}\right)\left\{-\left(I_2+I_3\right)\frac{\mathrm{d}^2\phi}{\mathrm{d}x^2}+H_{44}\left(\phi+\frac{\mathrm{d}w}{\mathrm{d}x}\right)\right\}=0 \tag{46}$$

It is quite clear that Eq. (44) is independent of Eqs. (45) and (46). Therefore, to compute the system's stability capacity Eqs. (45) and (46) will be solved. It is vital to remember that if we consider $\mu = l$ or $\mu = 0, l = 0$, the local analysis is performed.

Now, the pre-buckling compressive axial forces can be written as

$$N_x^0 = N^{\mathrm{Mech}} + N^{\mathrm{Mag}} \tag{47}$$

for which one can dedicate the magnetic and mechanical parts as N^{Mag} and N^{Mech} respectively.

$$N^{\mathrm{Mech}} = -P_{\mathrm{cr}} \tag{48}$$

$$N^{\mathrm{Mag}} = -q_{31}\psi \tag{49}$$

3 Solution process

Buckling equations are solved based on various methods. In between these solution techniques well-known ones can refer to the Galerkin weighted residual method (GWRM) which is a simple one involving a fast solution time [56]. To proceed with this method, the unknown functions $w\,(x)$ and $\phi\,(x)$ can be chosen as

$$w\,(x) = \sum_{m=1}^{N} a_m\,(x) \tag{50}$$

$$\phi\,(x) = \sum_{m=1}^{N} b_m\,(x) \tag{51}$$

The existed functions $a_m\,(x)$ and $b_m\,(x)$ based on the GWRM are expanded as

$$a_m = \int_0^L W_m\,(x)\,X_m \mathrm{d}x \tag{52}$$

$$b_m = \int_0^L \Phi_m\,(x)\,X_m \mathrm{d}x \tag{53}$$

Pertained to simple end conditions (SS), W_m and Φ_m are trigonometric functions as

$$W_m\,(x) = \sin\left(\frac{\pi}{L}x\right) \tag{54}$$

$$\Phi_m\,(x) = \cos\left(\frac{\pi}{L}x\right) \tag{55}$$

Manipulating and simplifying Eqs. (45) and (46) and combining it with Eq. (23), then based on Eqs. (50) and (51) and associating $m = 1$, the linear analytical stability equation of the PFM beam-like nano solid can be achieved.

4 Discussion and numerical results

4.1 Results validation

The verification section is here conducted to devote the exactness of the solution process. This part of the study is divided into two divisions. The first validation (Table 1) corresponds to Euler–Bernoulli (EB) and Timoshenko (TB) common nanobeams based on nonlocal effects only. The TB results are then compared with the EB ones in Table 2 owing to the PFM nanoscale beams by comparing results of EB small size beam with TB on the basis of substituting physical quantities in Table 3 [43,44].

The listed results in Table 1 represent that the difference between TB with EB tends to be shorter while increasing the value of the nonlocal parameter. What is more, no one can see any conflicts between present TB with those of [76]. In another investigation adjusted by Table 2, it is mentionable that the difference between the stability amounts of TB versus EB has become smaller. This smaller difference is observed while μ is increasing and the structure is PFM. In fact, the nonlocal parameter effect except decreasing the stiffness of the nanostructure deactivates the influence of shear deformations and then brings the EB and TB close to each other. Ultimately, on the basis of these prepared tables, one can say that a very good accuracy and agreement are revealed for the employed solving technique.

4.2 Buckling analysis

In this article, the static linear buckling analysis of a piezo-flexomagnetic (PFM) nanobeam is probed to understand the flexomagnetic property more We will determine the effectiveness of FM for a shear deformable structure in the ultrasmall size. The values of small scale parameters have been gotten as $0.5\,\text{nm} < e_0a < 0.8\,\text{nm}$ [77], and $0 < e_0a \leqslant 2\,\text{nm}$ [78,79]. The value of the strain gradient parameter has been estimated as same as the lattice number of the examined nanostructure as $l = 1\,\text{nm}$.

In the results section, by maneuvering on the dimensionless relationship of length to beam thickness (L/h), we try to evaluate the difference between the results of EB and TB beams in both local and nonlocal phases. Since this dimensionless ratio directly determines the importance of shear deformations (it was seen that in small values of this coefficient, the beam is thicker and the shear deformations are further important), the aim is to determine the effect of shear deformations on beams with FM property to know whether FM will be more important considering the shear deformation.

First, in order to evaluate the different cases, Figs. 2 and 3 represent the problem by focusing on the nonlocal parameter and the strain gradient, respectively. With the help of Fig. 2, it is quite obvious that the thinner the beam, the less important the shear deformation in the smart beam. However, the process of reducing the results in the local beam ($e_0a = 0$) will be on a steep slope. In fact, the nonlocal parameter and the shear deformation effect directly impressed each other. When the value of the nonlocal coefficient is other than zero ($e_0a = 2\text{nm}$), the difference between the results of EB and TB decreases. Thus, it can be stated that the local solution ($e_0a = 0$) of the nanostructures will lead to a more gap in the difference between the results of EB and TB. In Fig. 3, it can be seen that by increasing the value of the strain gradient parameter, the stiffer the material, the greater the difference between the EB and TB results. From these two diagrams, it can be concluded that the stiffer the material and its structure, the more important the shear deformations seem.

Figure 4 is based on changes in the value of the strain gradient parameter. Both EB and TB consist of two modes. The first mode is the PM beam and the second mode is the PFM beam. The result of the critical load for the EB-PFM at $l = 0$ is 2.836 nN and at $l = 2\text{nm}$ is 3.6876 nN. Also for TB-PFM is 2.7757 nN and 3.6055 nN, respectively. But we see that for PM beam in EB mode is 2.7373 nN and 3.5889 nN, respectively, and in TB mode is 2.6821 nN and 3.5119 nN. Therefore, considering the large values of the strain gradient parameter, we see that the difference between the results of EB-PM and TB-PM will be less than those of the EB-PFM with TB-PFM. It can be said that the strain gradient parameter affects the PFM beam more than the PM beams. A physical reason may be that the piezo-flexomagnetic material is stiffer than the piezo material.

According to Fig. 5, we have tried to compare EB and TB in piezo and piezo-flexomagnetic modes by considering the numerical changes of the slenderness parameter (L/h). For this purpose, we assessed the beam in the thicker zone. It shall be reminded that the results of TB are not accurate enough in the very thick range, and TB theory is often suitable for beams with $6 <$ L/h, and also in the case of EB for $10 <$ L/h. According to the diagram and in the thicker mode of the beams, it is observed that the critical load for the EB-PM beam is 12.615 nN and for the TB-PM is 11.471 nN, in contrast to EB-PFM is 13.009 nN and for

Table 1 Comparison of critical buckling load ($C_{11} = 1\,\text{TPa}, \upsilon = 0.3, \text{l} = 0\,\text{nm}, \psi = 0\,\text{mA}$ SS, $\overline{P_{rmCr}} = \frac{P_{\text{Cr}} L^2}{C_{11} I_c}$)

$\overline{P_{\text{Cr}}}$										
L/h	$e_0a = 0\,\text{nm}$		$e_0a = 0.5\,\text{nm}$		$e_0a = 1\,\text{nm}$		$e_0a = 1.5\,\text{nm}$		$e_0a = 2\,\text{nm}$	
	EB [76], TB [76]	TB-Present	EB [76], TB [76]	TB-Present	EB [76], TB [76]	TB-Present	EB [76], TB [76]	TB-Present	EB [76], TB [76]	TB-Present
10	2.4674	2.4056	2.4079	2.3477	2.2457	2.1895	2.0190	1.9685	1.7690	1.7247
	2.4056		2.3477		2.1895		1.8685		1.7247	
30	2.4674	2.4603	2.4606	2.4536	2.4406	2.4336	2.4079	2.4011	2.3637	2.3569
	2.4603		2.4536		2.4336		2.4011		2.3569	

Table 2 Comparison of the critical buckling load of the piezomagnetic-flexomagnetic CFO nanostructure for EB and TB ($l = 1\,\text{nm}$, $\psi = 1\,\text{mA}$, SS)

P_{Cr} (nN)						
L/h	$\mu = 0\,\text{nm}^2$		$\mu = 1\,\text{nm}^2$		$\mu = 2\,\text{nm}^2$	
	EB	TB	EB	TB	EB	TB
10	3.2828	3.2111	3.0489	2.9832	2.8536	2.7928
12	2.4074	2.3734	2.2946	2.2627	2.1954	2.1652
14	1.9007	1.8825	1.8398	1.8225	1.7845	1.7679
16	1.5803	1.5697	1.5446	1.5344	1.5115	1.5016
18	1.3645	1.3579	1.3422	1.3358	1.3212	1.3150
20	1.2121	1.2078	1.1974	1.1933	1.1835	1.1794
22	1.1003	1.0974	1.0903	1.0875	1.0807	1.0779
24	1.0159	1.0139	1.0089	1.0069	1.0021	1.0001
26	0.9506	0.9491	0.9455	0.9440	0.9405	0.9390
28	0.8990	0.8978	0.8951	0.8941	0.8914	0.8903
30	0.8575	0.8566	0.8546	0.8537	0.8517	0.8509

Table 3 Properties of the magnetic nanoparticle

$CoFe_2O_4$ (CFO)
$C_{11} = 286\,\text{GPa}$
$\nu = 0.32$
$q_{31} = 580.3\,\text{N/A m}$
$a_{33} = 1.57 \times 10^{-4}\,\text{N/A}^2$
A = Ampere

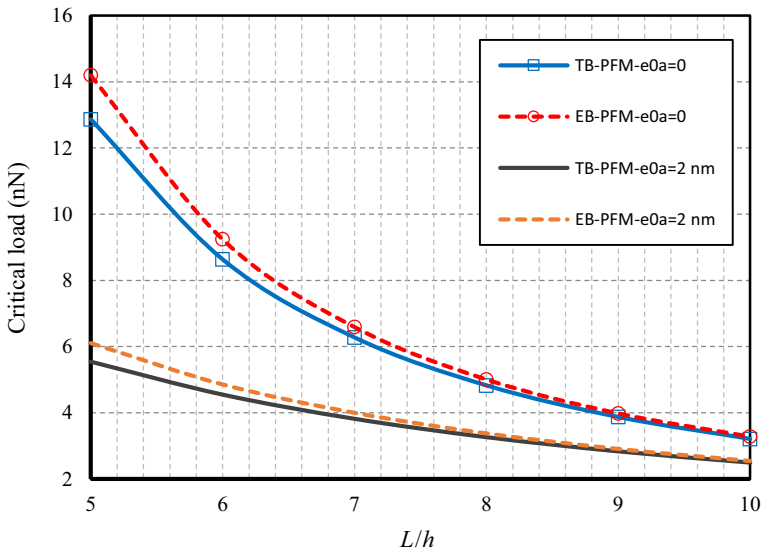

Fig. 2 Nonlocal parameter versus EB and TB for COF nanostructure ($l = 1\,\text{nm}$, $\psi = 1\,\text{mA}$)

TB-PFM beam is 11.793 nN. Therefore, it can be stated that the difference between the results of EB and TB in piezo-flexomagnetic mode is greater than those of piezomagnetic mode. Of course, the literature [43,52] reported that FM is dominant in thinner structures. However, as a result of this study, one can conclude that the flexomagnetic effect will lead to the greater importance of shear deformations in thicker nanobeams.

Figure 6 is drawn to show a pure mechanical response of the nanoscale beam (NB) compared with PM and PFM for both EB and TB. The NB excludes magnetic and also the FM properties. It is tried to sketch the beams from a thick beam up to a moderately thick beam. As seen, the NB has the least mechanical stability in comparison with the PM and PFM nanobeams. Interestingly, in an analogy between NB with PFM, and PM, it can be observed that the results of the EB-NB would be matched with those of TB-NB sooner than other

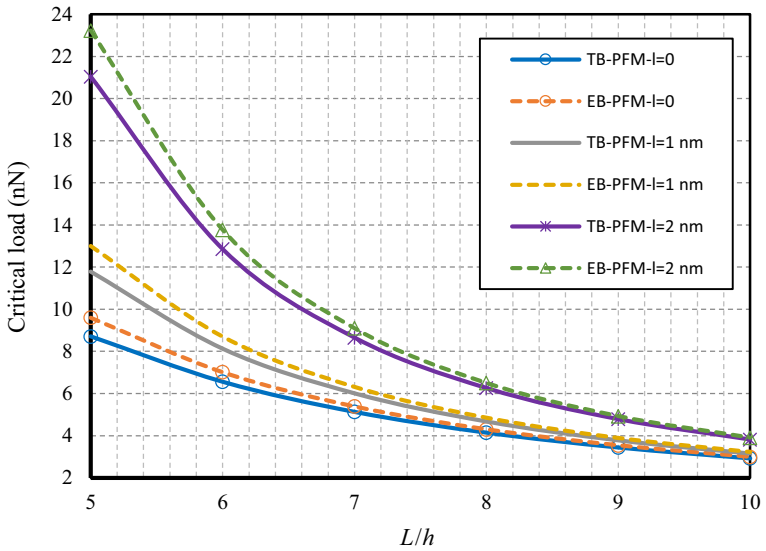

Fig. 3 Strain gradient parameter versus EB and TB for COF nanostructure ($ea = 0.5$ nm, $\psi = 1$ mA)

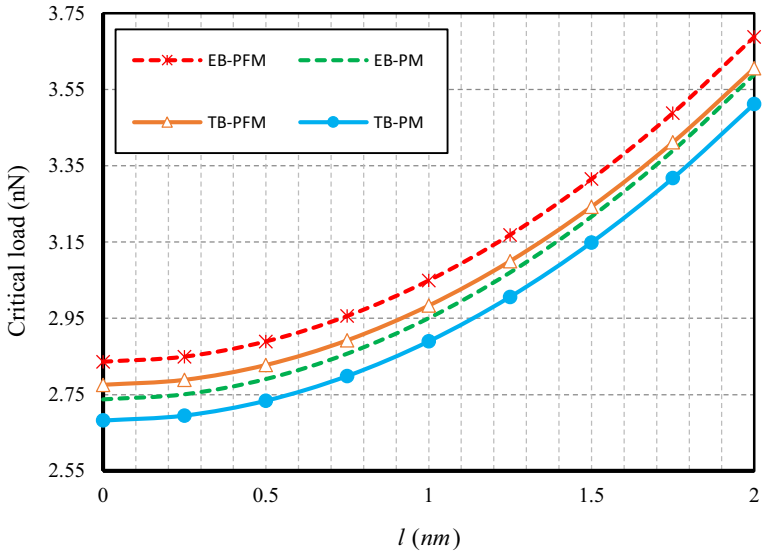

Fig. 4 Strain gradient parameter versus EB and TB for COF nanostructure ($ea = 1$ nm, $L = 10$ h, $\psi = 1$ mA)

cases. From L/h $= 11$, the results of EB and TB for NB are so closed to each other. However, this does not apply to magnetic cases. It means the importance of shear deformation will be increased in piezomagnetic-flexomagnetic domains.

5 Conclusions

This work aimed to extend the shear deformation effect on the flexomagneticity response of a piezomagnetic ultrasmall scale elastic beam. We established the governing equations by using the Timoshenko beam. The nonlocal mechanics of the nanobeam was concerned with the nonlocal strain gradient approach by which we are able to transfer the discretize atomic lattice into a continuum region. The solution of the obtained equations corresponded to a closedform solution within which the numerical results were reported for simply supported end support. We organized some tabulated verifications to corroborate the numerical results. Based on the

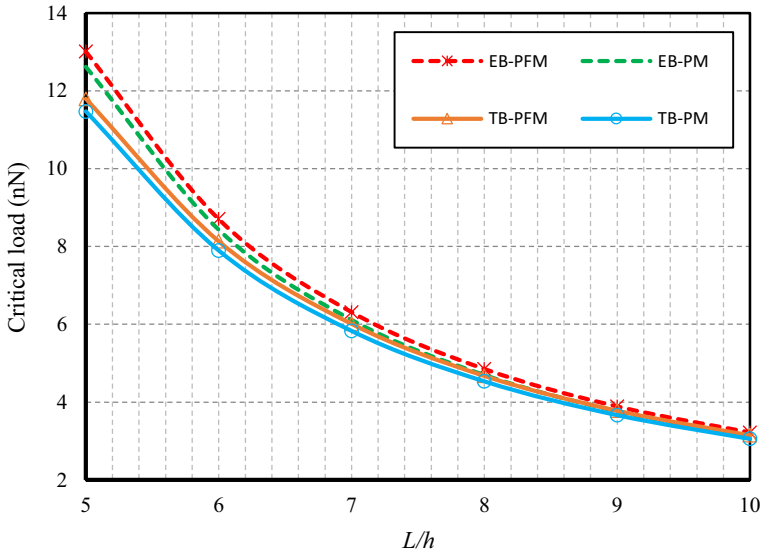

Fig. 5 Slenderness ratio versus EB and TB for COF nanostructure ($l = 1$ nm, $ea = 0.5$ nm, $\psi = 1$ mA)

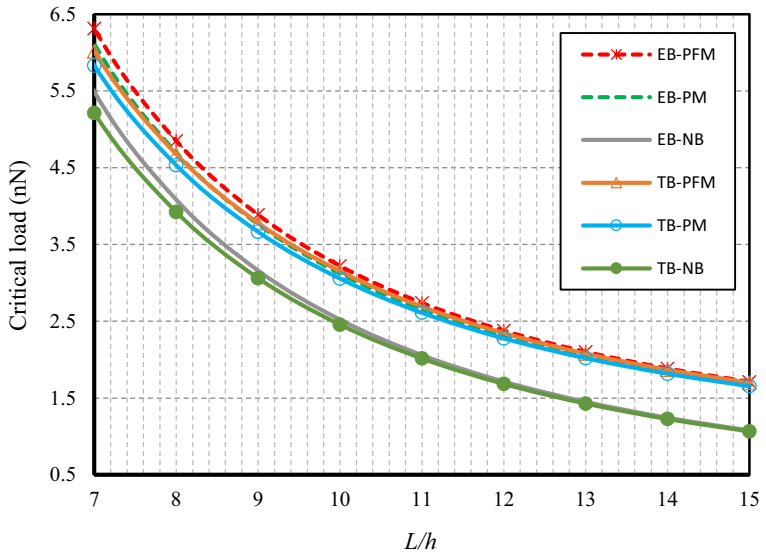

Fig. 6 Slenderness ratio versus EB and TB for different nanostructure ($l = 1$ nm, $ea = 0.5$ nm, $\psi = 1$ mA)

detailed parametric study and from an engineering perspective, this work provides some new attainments and outcome remarks as

- The stiffer structure leads to the further remarkable of shear deformations
- The lesser the values of the nonlocal parameter, the more marked the shear deformations
- The larger the values of the strain gradient parameter, the more considerable the shear deformations
- For the smart nanobeams, the FM will affect the existence of shear deformations and the effect is to increase its importance.

Acknowledgements V.A. Eremeyev acknowledges the support of the Government of the Russian Federation (contract No. 14.Z50.31.0046).

References

1. Diandra, L.L.-P., Rieke, R.D.: Magnetic properties of nanostructured materials. Chem. Mater. **8**, 1770–1783 (1996)
2. Fei, C., Zhang, Y., Yang, Z., Liu, Y., Xiong, R., Shi, J., Ruan, X.: Synthesis and magnetic properties of hard magnetic (CoFe2O4)-soft magnetic (Fe3O4) nano-composite ceramics by SPS technology. J. Magn. Magn. Mater. **323**, 1811–1816 (2011)
3. Reddy, V.A., Pathak, N.P., Nath, R.: Particle size dependent magnetic properties and phase transitions in multiferroic BiFeO3 nano-particles. J. Alloys Compd. **543**, 206–212 (2012)
4. Karimi, Z., Mohammadifar, Y., Shokrollahi, H., Khameneh Asl, S., Yousefi, G., Karimi, L.: Magnetic and structural properties of nano sized Dy-doped cobalt ferrite synthesized by co-precipitation. J. Magn. Magn. Mater. **361**, 150–156 (2014)
5. Obaidat, I., Bashar, I., Haik, Y.: Magnetic properties of magnetic nanoparticles for efficient hyperthermia. Nanomaterials **5**, 63–89 (2015)
6. Rajath, P.C., Manna, R.S., Banerjee, D., Varma, M.R., Suresh, K.G., Nigam, A.K.: Magnetic properties of CoFe2O4 synthesized by solid state, citrate precursor and polymerized complex methods: a comparative study. J. Alloys Compd. **453**, 298–303 (2008)
7. Wang, J., Deng, T., Dai, Y.: Comparative study on the preparation procedures of cobalt ferrites by aqueous processing at ambient temperatures. J. Alloys Compd. **419**, 155–161 (2006)
8. Khandekar, M.S., Kamble, R.C., Patil, J.Y., Kolekar, Y.D., Suryavanshi, S.S.: Effect of calcination temperature on the structural and electrical properties of cobalt ferrite synthesized by combustion method. J. Alloys Compd. **509**, 1861–1865 (2011)
9. Kim, D.H., Nikles, D.E., Johnson, D.T., Brazel, C.S.: Heat generation of aqueously dispersed CoFe2O4 nanoparticles as heating agents for magnetically activated drug delivery and hyperthermia. J. Magn. Magn. Mater. **320**, 2390–2396 (2008)
10. Morais, P.C.: Photoacoustic spectroscopy as a key technique in the investigation of nanosized magnetic particles for drug delivery systems. J. Alloys Compd. **483**, 544–548 (2009)
11. Deraz, N.M.: Glycine-assisted fabrication of nanocrystalline cobalt ferrite system. J. Anal. Appl. Pyrol. **88**, 103–109 (2010)
12. Kabychenkov, A.F., Lisovskii, F.V.: Flexomagnetic and flexoantiferromagnetic effects in centrosymmetric antiferromagnetic materials. Tech. Phys. **64**, 980–983 (2019)
13. Eliseev, E.A., Morozovska, A.N., Glinchuk, M.D., Blinc, R.: Spontaneous flexoelectric/flexomagnetic effect in nanoferroics. Physical Review B **79**, 165433 (2009)
14. Lukashev, P., Sabirianov, R.F.: Flexomagnetic effect in frustrated triangular magnetic structures. Phys. Rev. B **82**, 094417 (2010)
15. Ma, W.: Flexoelectricity: strain gradient effects in ferroelectrics. Phys. Scr. **129**, 180–183 (2007)
16. Lee, D., Yoon, A., Jang, S.Y., Yoon, J.-G., Chung, J.-S., Kim, M., Scott, J.F., Noh, T.W.: Giant flexoelectric effect in ferroelectric epitaxial thin films. Phys. Rev. Lett. **107**, 057602 (2011)
17. Nguyen, T.D., Mao, S., Yeh, Y.-W., Purohit, P.K., McAlpine, M.C.: Nanoscale flexoelectricity. Adv. Mater. **25**, 946–974 (2013)
18. Zubko, P., Catalan, G., Tagantsev, A.K.: Flexoelectric effect in solids. Annu. Rev. Mater. Res. **43**, 387–421 (2013)
19. Yudin, P.V., Tagantsev, A.K.: Fundamentals of flexoelectricity in solids. Nanotechnology **24**, 432001 (2013)
20. Yurkov, A.S., Tagantsev, A.K.: Strong surface effect on direct bulk flexoelectric response in solids. Appl. Phys. Lett. **108**, 022904 (2016)
21. Wang, B., Gu, Y., Zhang, S., Chen, L.-Q.: Flexoelectricity in solids: progress, challenges, and perspectives. Prog. Mater Sci. **106**, 100570 (2019)
22. Cross, L.: Flexoelectric effects: charge separation in insulating solids subjected to elastic strain gradients. J. Mater. Sci. **41**, 53–63 (2006)
23. Ma, W., Cross, L.E.: Observation of the flexoelectric effect in relaxor $Pb(Mg_{1/3}Nb_{2/3})O_3$ ceramics. Appl. Phys. Lett. **78**, 2920–21 (2001)
24. Ma, W., Cross, L.E.: Flexoelectricity of barium titanate. Appl. Phys. Lett. **88**, 232902 (2006)
25. Zubko, P., Catalan, G., Buckley, A., Welche, P.R.L., Scott, J.F.: Strain-gradient-induced polarization in SrTiO3 single crystals. Phys. Rev. Lett. **99**, 167601 (2007)
26. Eremeyev, V.A., Ganghoffer, J.-F., Konopinska-Zmysłowska, V., Uglov, N.S.: Flexoelectricity and apparent piezoelectricity of a pantographic micro-bar. Int. J. Eng. Sci. **149**, 103213 (2020)
27. Esmaeili, M., Tadi Beni, Y.: Vibration and buckling analysis of functionally graded flexoelectric smart beam. J. Appl. Comput. Mech. **5**, 900–917 (2019)
28. Malikan, M., Eremeyev, V.A.: On the dynamics of a visco-piezo-flexoelectric nanobeam. Symmetry **12**, 643 (2020)
29. Singhal, A., Sedighi, H.-M., Ebrahimi, F., Kuznetsova, I.: Comparative study of the flexoelectricity effect with a highly/weakly interface in distinct piezoelectric materials (PZT-2, PZT-4, PZT-5H, LiNbO3, BaTiO3). Waves Random Compl. Media (2019). https://doi.org/10.1080/17455030.2019.1699676
30. Mawassy, N., Reda, H., Ganghoffer, J.-F., Eremeyev, V.A., Lakiss, H.: A variational approach of homogenization of piezoelectric composites towards piezoelectric and flexoelectric effective media. Int. J. Eng. Sci. **158**, 103410 (2021)
31. Ebnali Samani, M.S., Tadi Beni, Y.: Size dependent thermo-mechanical buckling of the flexoelectric nanobeam. Mater. Res. Express **5**, 085018 (2018)
32. Ghobadi, A., Tadi Beni, Y., Golestanian, H.: Nonlinear thermo-electromechanical vibration analysis of size-dependent functionally graded flexoelectric nano-plate exposed magnetic field. Arch. Appl. Mech. **90**, 2025–2070 (2020)
33. Ghobadi, A., Tadi Beni, Y., Golestanian, H.: Size dependent thermo-electro-mechanical nonlinear bending analysis of flexoelectric nano-plate in the presence of magnetic field. Int. J. Mech. Sci. **152**, 118–137 (2019)
34. Arefi, M., Zenkour, A.M.: Thermo-electro-magneto-mechanical bending behavior of size-dependent sandwich piezomagnetic nanoplates. Mech. Res. Commun. **84**, 27–42 (2017)
35. Ebrahimi, F., Barati, M.R.: Porosity-dependent vibration analysis of piezo-magnetically actuated heterogeneous nanobeams. Mech. Syst. Signal Process. **93**, 445–459 (2017)

36. Zenkour, A.M., Arefi, M., Alshehri, N.A.: Size-dependent analysis of a sandwich curved nanobeam integrated with piezomagnetic face-sheets. Results Phys. **7**, 2172–2182 (2017)
37. Sun, X.-P., Hong, Y.-Z., Dai, H.-L., Wang, L.: Nonlinear frequency analysis of buckled nanobeams in the presence of longitudinal magnetic field. Acta Mech. Solida Sin. **30**, 465–473 (2017)
38. Balasubramanian, K.R., Sivapirakasam, S.P., Anand, R.: Linear buckling and vibration behavior of piezoelectric/piezomagnetic beam under uniform magnetic field. Appl. Mech. Mater. **592–594**, 2071–2075 (2014)
39. Alibeigi, B., Beni, Y.T.: On the size-dependent magneto/electromechanical buckling of nanobeams. Eur. Phys. J. Plus **133**, 398 (2018)
40. Arefi, M., Kiani, M., Civalek, O.: 3-D magneto-electro-thermal analysis of layered nanoplate including porous core nanoplate and piezomagnetic face-sheets. Appl. Phys. A **126**, 76 (2020)
41. Saadatfar, M.: Stress redistribution analysis of piezomagnetic rotating thick-walled cylinder with temperature-and moisture-dependent material properties. J. Appl. Comput. Mech. **6**, 90–104 (2020)
42. Marin, M., Öchsner, A.: An initial boundary value problem for modeling a piezoelectric dipolar body. Contin. Mech. Thermodyn. **30**, 267–278 (2018)
43. Sidhardh, S., Ray, M.C.: Flexomagnetic response of nanostructures. J. Appl. Phys. **124**, 244101 (2018)
44. Zhang, N., Zheng, Sh, Chen, D.: Size-dependent static bending of flexomagnetic nanobeams. J. Appl. Phys. **126**, 223901 (2019)
45. Malikan, M., Eremeyev, V.A.: Free vibration of flexomagnetic nanostructured tubes based on stress-driven nonlocal elasticity, analysis of shells, plates, and beams. Adv. Struct. Mater. **134**, 215–226 (2020)
46. Malikan, M., Eremeyev, V.A.: On the geometrically nonlinear vibration of a piezo-flexomagnetic nanotube. Math. Methods Appl. Sci. (2020). https://doi.org/10.1002/mma.6758
47. Malikan, M., Eremeyev, V.A.: On nonlinear bending study of a piezo-flexomagnetic nanobeam based on an analytical-numerical solution. Nanomaterials **10**, 1762 (2020)
48. Malikan, M., Uglov, N.S., Eremeyev, V.A.: On instabilities and post-buckling of piezomagnetic and flexomagnetic nanostructures. Int. J. Eng. Sci. **157**, 10339 (2020)
49. Malikan, M., Wiczenbach, T., Eremeyev, V.A.: On thermal stability of piezo-flexomagnetic microbeams considering different temperature distributions. Contin. Mech. Thermodyn. (2021). https://doi.org/10.1007/s00161-021-00971-y
50. Malikan, M., Eremeyev, V.A., Żur, K.K.: Effect of axial porosities on flexomagnetic response of in-plane compressed piezomagnetic nanobeams. Symmetry **12**, 1935 (2020). https://doi.org/10.3390/sym12121935
51. Malikan, M., Eremeyev, V.A.: Flexomagnetic response of buckled piezomagnetic composite nanoplates. Compos. Struct. **267**, 113932 (2021)
52. Malikan, M., Eremeyev, V.A.: Effect of surface on the flexomagnetic response of ferroic composite nanostructures; nonlinear bending analysis. Compos. Struct. **271**(114179) (2021). https://doi.org/10.1016/j.compstruct.2021.114179
53. Reddy, J.N.: Nonlocal nonlinear formulations for bending of classical and shear deformation theories of beams and plates. Int. J. Eng. Sci. **48**, 1507–1518 (2010)
54. She, G.-L., Liu, H.-B., Karami, B.: Resonance analysis of composite curved microbeams reinforced with graphene nanoplatelets. Thin-Walled Struct. **160**, 107407 (2021)
55. Malikan, M., Eremeyev, V.A., Sedighi, H.M.: Buckling analysis of a non-concentric double-walled carbon nanotube. Acta Mech. (2020). https://doi.org/10.1007/s00707-020-02784-7
56. Malikan, M., Eremeyev, V.A.: A new hyperbolic-polynomial higher-order elasticity theory for mechanics of thick FGM beams with imperfection in the material composition. Compos. Struct. **249**, 112486 (2020)
57. Turco, E.: Numerically driven tuning of equilibrium paths for pantographic beams. Contin. Mech. Thermodyn. **31**, 1941–1960 (2019)
58. Marin, M., Öchsner, A., Taus, D.: On structural stability for an elastic body with voids having dipolar structure. Contin. Mech. Thermodyn. **32**, 147–160 (2020)
59. Malikan, M.: Electro-thermal buckling of elastically supported double-layered piezoelectric nanoplates affected by an external electric voltage. Multi. Model. Mater. Struct. **15**, 50–78 (2019)
60. Malikan, M.: Temperature influences on shear stability of a nanosize plate with piezoelectricity effect. Multi. Model. Mater. Struct. **14**, 125–142 (2018)
61. Lim, C.W., Zhang, G., Reddy, J.N.: A higher-order nonlocal elasticity and strain gradient theory and its applications in wave propagation. J. Mech. Phys. Solids **78**, 298–313 (2015)
62. Lam, D.C.C., Yang, F., Chong, A.C.M., Wang, J., Tong, P.: Experiments and theory in strain gradient elasticity. J. Mech. Phys. Solids **51**, 1477–1508 (2003)
63. Ansari, R., Sahmani, S., Arash, B.: Nonlocal plate model for free vibrations of single-layered graphene sheets. Phys. Lett. A **375**, 53–62 (2010)
64. Akbarzadeh Khorshidi, M.: The material length scale parameter used in couple stress theories is not a material constant. Int. J. Eng. Sci. **133**, 15–25 (2018)
65. Yang, H., Timofeev, D., Giorgio, I., et al.: Effective strain gradient continuum model of metamaterials and size effects analysis. Contin. Mech. Thermodyn. (2020). https://doi.org/10.1007/s00161-020-00910-3
66. Abali, B.E.: Revealing the physical insight of a length-scale parameter in metamaterials by exploiting the variational formulation. Contin. Mech. Thermodyn. **31**, 885–894 (2019)
67. Karami, B., Shahsavari, D., Janghorban, M., Li, L.: On the resonance of functionally graded nanoplates using bi-Helmholtz nonlocal strain gradient theory. Int. J. Eng. Sci. **144**, 103143 (2019)
68. Malikan, M., Nguyen, V.B., Tornabene, F.: Damped forced vibration analysis of single-walled carbon nanotubes resting on viscoelastic foundation in thermal environment using nonlocal strain gradient theory. Eng. Sci. Technol. Int. J. **21**, 778–786 (2018)
69. Malikan, M., Dimitri, R., Tornabene, F.: Transient response of oscillated carbon nanotubes with an internal and external damping. Compos. B Eng. **158**, 198–205 (2019)

70. Malikan, M., Krasheninnikov, M., Eremeyev, V.A.: Torsional stability capacity of a nano-composite shell based on a nonlocal strain gradient shell model under a three-dimensional magnetic field. Int. J. Eng. Sci. **148**, 103210 (2020)
71. Kumar Jena, S., Chakraverty, S., Tornabene, F.: Dynamical behavior of nanobeam embedded in constant, linear, parabolic, and sinusoidal types of Winkler elastic foundation using first-Order nonlocal strain gradient model. Mater. Res. Express **6**, 0850f2 (2019)
72. Malikan, M., Eremeyev, V.A.: Post-critical buckling of truncated conical carbon nanotubes considering surface effects embedding in a nonlinear Winkler substrate using the Rayleigh–Ritz method. Mater. Res. Express **7**, 025005 (2020)
73. Karami, B., Janghorban, M., Rabczuk, T.: Dynamics of two-dimensional functionally graded tapered Timoshenko nanobeam in thermal environment using nonlocal strain gradient theory. Compos. B Eng. **182**, 107622 (2020)
74. Sahmani, S., Safaei, B.: Nonlocal strain gradient nonlinear resonance of bi-directional functionally graded composite micro/nano-beams under periodic soft excitation. Thin-Walled Struct. **143**, 106226 (2019)
75. Fan, F., Safaei, B., Sahmani, S.: Buckling and postbuckling response of nonlocal strain gradient porous functionally graded micro/nano-plates via NURBS-based isogeometric analysis. Thin-Walled Struct. **159**, 107231 (2021)
76. Simsek, M., Yurtcu, H.H.: Analytical solutions for bending and buckling of functionally graded nanobeams based on the nonlocal Timoshenko beam theory. Compos. Struct. **9**, 378–386 (2013)
77. Ansari, R., Sahmani, S., Rouhi, H.: Rayleigh-Ritz axial buckling analysis of single-walled carbon nanotubes with different boundary conditions. Phys. Lett. A **375**, 1255–1263 (2011)
78. Duan, W.H., Wang, C.M.: Exact solutions for axisymmetric bending of micro/nanoscale circular plates based on nonlocal plate theory. Nanotechnology **18**, 385704 (2007)
79. Duan, W.H., Wang, C.M., Zhang, Y.Y.: Calibration of nonlocal scaling effect parameter for free vibration of carbon nanotubes by molecular dynamics. J. Appl. Phys. **101**, 24305 (2007)